

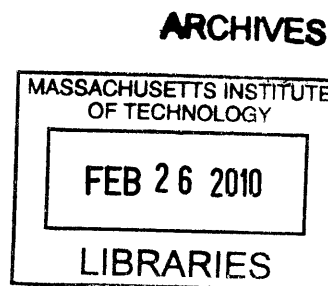
Experimental Methods to Examine the Role of Vibrational Excitation in the Singlet-Triplet Spin-Orbit Coupling in Acetylene

by

Erika Marie Robertson

B.S., Chemistry (2007)
B.S., Mathematics (2007)

Indiana University, Bloomington



Submitted to the Department of Chemistry in Partial Fulfillment of the
Requirements for the Degree of Master of Science in Chemistry

at the

Massachusetts Institute of Technology

February 2010

© 2010 Massachusetts Institute of Technology
All rights reserved

Signature of Author ...
.....
Department of Chemistry
November 23, 2009

Certified by
.....
Robert W. Field
Haslam and Dewey Professor of Chemistry
Thesis Supervisor

Accepted by
.....
Robert W. Field
Chairman, Department Committee on Graduate Theses

Experimental Methods to Examine the Role of Vibrational Excitation in the Singlet-Triplet Spin-Orbit Coupling in Acetylene

by

Erika Marie Robertson

Submitted to the Department of Chemistry on November 23, 2009 in Partial Fulfillment of the Requirements of the Degree of Master of Science in Chemistry

ABSTRACT

Despite being a seemingly simple molecule, acetylene has a complicated electronic structure that has been studied extensively both experimentally and theoretically. Acetylene has been observed to have a complex spin-orbit coupling mechanism where the first excited singlet state S_1 couples to the triplet state T_3 which is then coupled to the dense manifold of vibrational states in the $T_{1,2}$ electronic states. A description of theories imperative to this study is provided and each is related to its application in experiment. A description of how to obtain important parameters in the coupling, such as the coupling strength, the singlet-triplet mixing fraction, the radiative lifetime, and the relative energy ordering and separation between the singlet and coupled triplet, is given. Finally, key vibrational levels of interest that should be investigated are described.

Thesis Supervisor: Robert W. Field

Title: Haslam and Dewey Professor of Chemistry

Table of Contents

Chapter 1: Introduction	5
1.1 Triplet State.....	5
1.2 Previous experimental work on acetylene.....	6
1.3 Previous theoretical work on acetylene.....	15
1.4 Vibrational Modes and Electronic Energy Levels of Acetylene.....	18
1.5 Objective of Thesis.....	21
Chapter 2: Spin-orbit coupling	23
2.1 Theory of spin-orbit coupling.....	23
2.2 Application to experiment.....	24
2.3 Method to access $J = K = N = 0$ states experimentally.....	25
Chapter 3: Radiative Lifetimes	27
3.1 Theory of radiative lifetimes.....	27
3.2 Application to experiments.....	28
Chapter 4: Zeeman effect	29
4.1 Theory of the Zeeman Effect.....	29
4.2 Quantum Beat Experiment.....	31
Chapter 5: Late-gated fluorescence	34
5.1 Guaranteed Crossings.....	34
5.2 Late-gated Fluorescence.....	36
Chapter 6: Experimental Details	37
6.1 Setup of apparatus.....	37
6.2 Application of theories to experiment.....	39

6.3 Choosing vibrational levels.....	40
Chapter 7: Conclusion	43
Bibliography	45

List of Figures

Figure 1.1: Energy levels for <i>cis</i> and <i>trans</i> isomers of the low-lying excited states of acetylene.....	17
Figure 1.2: Vibrational modes of the ground state of acetylene.....	19
Figure 1.3: Vibrational modes of the first excited singlet state of acetylene.....	20
Figure 2.1: Spin-orbit Matrix Elements in Terms of the J and K Quantum Numbers of the Singlet State.....	23
Figure 6.1: Experimental Apparatus.....	37

Chapter 1: Introduction

1.1 Triplet States

Triplet states are states of molecules or atoms that have the spin angular momentum quantum number S equal to 1. The term “triplet” comes from the spin multiplicity, $2S+1$, which is equal to 3 for a triplet state. Most operators in quantum mechanics, especially those governing transition probabilities, are diagonal in S , so the $\Delta S=0$ rule makes triplet states not normally accessible from the ground singlet state. Likewise, since molecules cannot easily fluoresce back to the ground state from the triplet state, triplet states are also very long lived. Because triplet states are normally highly energetic excited states of the molecule and because they are metastable, they are particularly important as possible reaction intermediates. Metastable triplet states can be thought of as long-lived packets of energy. A triplet state is similar to a free radical in that it has two (rather than one for a free radical) unpaired electrons, making it highly reactive. For example, the triplet state of photosystem II reaction centers plays an important role as a reaction intermediate in electron-transfer events during photosynthesis [14].

The phenomenon of phosphorescence, the emission of light from a molecule or atom at a delayed time (on the order of milliseconds to seconds) relative to excitation, was first observed in organic molecules in rigid glass solutions. It was observed that the phosphorescence was from a metastable (long-lived) state of the molecule and was observed in several dye molecules [22]. However, there was initially much controversy over the nature of this metastable state [22]. Even Jablonski, the creator of the Jablonski diagram used to illustrate electronic energy levels of molecules and intersystem crossing,

did not believe that triplet states actually existed [22]; he insisted that the metastable states observed in phosphorescence were singlet states having a very small probability of excitation. In 1941, Lewis *et. al.* proposed that the metastable state observed to phosphoresce in an acid fluorescein dye was a triplet state [26]. Some doubt remained, however, to the identity of the metastable state due to the fact that phosphorescence had only been observed in glass solutions. In 1944 Lewis and Kasha analyzed the spectra of 89 molecules to prove the generality of the phenomenon of phosphorescence and to unambiguously assign the metastable states as triplets [25]. Today triplet states are routinely observed in numerous molecules.

1.2 Previous Experimental Work on Acetylene

Acetylene (C_2H_2) is one of the smallest polyatomic organic molecules. This makes it ideal for use as a model upon which to build knowledge of larger systems. Acetylene also has a triple bond which makes it useful for modeling and understanding pi-bonding. Acetylene has a symmetrical geometric structure and a relatively simple rotation-vibration-electronic structure, which allows application of well-known theories of analysis from diatomic molecules, while adding the extra complexity of multiple vibrational modes found in polyatomic molecules.

Acetylene is linear in its ground state. However, in 1952 Ingold and King recorded the first near-ultraviolet absorption spectrum of the first excited singlet state of acetylene and determined that it must be *trans*-bent in geometry with 1A_u symmetry [23, 19]. This was the first observation of a qualitative change in molecular geometry upon electronic excitation of any molecule. In 1954 Innes performed a higher resolution study

of the absorption spectrum of acetylene and confirmed the excited singlet state to be *trans*-bent [20].

In addition to its singlet states, the triplet states of acetylene have been studied extensively. In 1972, Burton and Hunziker [6] made the first spectroscopic observation of triplet acetylene. They used mercury photosensitization (collision of acetylene with electronically excited mercury atoms) to produce excited state triplet acetylene. Previous mercury photosensitization studies had shown that this process leads to acetylene polymerization. However, this polymerization could be suppressed by the presence of NO. Since NO is a radical, inhibition of polymerization by NO led Burton and Hunziker to suspect a free radical mechanism. However they also observed that the yield of molecular hydrogen decreased as the amount of acetylene increased. This meant that the acetylene intermediate produced could not be a free radical but had to be an electronically excited state of acetylene. These results led them to postulate that the process was creating triplet state acetylene. They were also able to estimate an energy bound on the triplet state of $2.7\text{eV} < T < 4.7\text{eV}$ by looking at various molecules and determining which were able to be quenched by triplet acetylene.

Five years later in 1979, Wendt, Hippler, and Hunziker carried out additional mercury photosensitization experiments on acetylene. Here they observed the near-infrared absorption spectrum and found it to be consistent with the $1^3A_2 - 1^3B_2$ triplet-triplet transition. This was the first experimental observation of the lowest triplet state in the *cis* conformation.

In 1976, Hemminger, Wicke, and Klemperer performed the first measurements on metastable acetylene produced by electron impact excitation of a beam of acetylene [17].

The resulting metastables were detected via Auger electron emission from a cesium surface. (The mechanism of this Auger emission was worked out by Hagstrom [16] and later explained in detail by Cunningham [7]. A metastable atom or molecule colliding with a metal surface may cause ejection of an electron by one of two possible mechanisms. In one case, deexcitation of the excited electron of the metastable species stimulated by interaction with its image transition moment in the metal fills the vacancy in the lower orbital of the metastable. The energy released by this relaxation excites a metal electron to a higher state in the band structure. If the energy in this metal electron exceeds the work function of the metal, the electron is released. In the second mechanism, an electron from the metal tunnels into the metastable, filling the vacancy in the lower orbital. The energy released from this process then further excites the already excited electron in the metastable. If the energy in this excited electron is larger than the ionization potential of the molecule, an electron is released.) In the Auger emission process, a metastable will only cause ejection of an electron from the surface if the metastable has its energy in electronic excitation. Thus molecules in highly excited vibrational states of the ground electronic state will not be detected. In continued work on electron impact experiments of acetylene, Lisy and Klemperer determined whether the electric dipole moment of the metastable is nonzero using an electrostatic quadrupole lens [27]. They found the molecule to be nonpolar and were able to conclude that the metastable state was in the *trans* geometry. This was the first observation of the *trans*-bent state. Observation of the *trans* state was made possible in this experiment because of the difference in spin-orbit perturbations between the *cis* and *trans* triplet state with highly vibrationally excited levels of the ground singlet state [29]. Spin-orbit coupling of

the *cis* state to highly excited vibrational levels of the ground state is only electronically allowed, while coupling of the *trans* state is only vibronically allowed. This difference causes low-lying vibrational states of the *cis* isomer to couple strongly to highly excited vibrational levels of the ground state. This makes the *cis* isomer less detectable through the Auger process because it has more singlet ground state vibrationally excited character than triplet electronically excited character. The *trans* isomer is still detected strongly because low-lying vibrational levels will not mix as strongly to the ground state because this spin-orbit perturbation is only vibronically allowed. The coupling of the *cis* state to the vibrational manifold of the ground state will also significantly reduce its ability to be deflected in an electric field, also decreasing its detectivity.

In addition to *cis* and *trans* geometry excited states, a third linear geometry is also possible. In 1997 Swiderick, Michaud, and Sanche used low-energy electron-energy-loss spectroscopy to observe the linear geometry triplet state in solid acetylene [40].

In 1982 Abramson, Kittrell, Kinsey, and Field carried out the first laser-induced fluorescence experiments on the \tilde{A} state of acetylene [2]. They observed unusually long lifetimes of 2-5 μ s, quantum beat modulations in the fluorescence decay, and “extra” lines of the singlet state, all indicating that the singlet state is mixing with a nearby triplet state. In 1985 Abramson, Field, Imre, Innes, and Kinsey expanded this work to stimulated emission pumping (SEP) experiments on acetylene [1, 39]. These experiments allowed the observation of a very large number of spectral features and allowed for population of highly excited vibrational levels of the ground S_0 state. Because of this large number of observed vibrational levels (much larger than the number that are Franck-Condon allowed), it can be seen that there is significant mixing due to

Fermi resonances and/or Coriolis coupling [1]. Fermi resonances occur when vibrational levels of the same symmetry are nearby in energy and are coupled by a nonzero anharmonic interaction term [4]. Coriolis coupling is a coupling between vibrational and rotational motion and occurs when two vibrational motions differ by a rotation about one of the principal axes of the molecule [4].

In 1986 Scherer, Chen, Redington, Kinsey, and Field performed fluorescence measurements on the \tilde{A} state of acetylene [35]. By analyzing the rotational structure of the spectrum, they hypothesized that the $3\nu_3$ vibrational level is perturbed by the $\nu_2 + 2\nu_4$ vibrational level via a Fermi resonance, although this assignment was incorrect. However, they also observed an anomalously large difference in the B and C rotational constants of the perturber, which led to the conclusion that this perturber level is also perturbed by a third level, probably $3\nu_4 + \nu_6$. This was an important step in thinking because it was the first suggestion that the perturber level is itself perturbed by a third level.

Ochi and Tsuchiya carried out the first Zeeman experiments on acetylene [33]. In the presence of a magnetic field, the initially degenerate laboratory fixed Z-axis projection of the spin quantum number, M_S , will split into three nondegenerate energy values. This effect is known as the Zeeman effect and will be described in further detail in Chapter 4. In the Ochi and Tsuchiya experiments, quantum beats were observed in the $3\nu_3$ level of the \tilde{A} state of acetylene. These quantum beats were attributed to two possible causes: 1) Zeeman splitting of the relevant level and 2) magnetic field-induced level anticrossing between the \tilde{A} state and a nearby triplet level [33].

Ochi and Tsuchiya expanded their work on acetylene to several vibrational levels of the \tilde{A} state ($n\nu_3$) [34]. They observed that for $n = 3,4$, the energy levels were split into several levels, while for $n = 2$, the levels were rarely split [34]. They also observed the lifetime of $3\nu_3$ to be relatively long compared to the other lower lying vibrational levels. This long lifetime, as well as observed large g-factors, caused them to propose that the $3\nu_3$ levels are coupling most efficiently to the triplet levels. They also propose a potential energy curve crossing between S_1 and T_3 which creates an indirect coupling between S_1 and T_2 through an S_1 - T_3 - T_2 coupling.

Peter Green, in collaboration with Patrick Dupré and Maurice Lombardi completed an extensive survey of the Zeeman Anticrossing Spectra of acetylene in the first excited singlet state with vibrational excitation $n\nu_3'$ ($n = 0-3$) [15] with a magnetic field strength of 0-8 T. Zeeman Anticrossing Spectra (ZAC) are recorded by measuring the fluorescence at a particular excitation wavelength and scanning the applied magnetic field. When two levels, one “bright” and the other one “dark, are Zeeman-tuned to near-degeneracy, the fluorescence intensity will dip due to the interaction between the two levels. Levels may be near-degenerate either accidentally or by a level being shifted by the magnetic field (Zeeman effect). In these experiments an increasing number of anticrossings were observed with increasing quanta in the ν_3 mode, with a particularly large number of crossings found at $3\nu_3$. Green also employed the Stark effect (shifting of levels by an electric field) in his experiments. By using the Zeeman and Stark effects, he was able to measure both the magnetic and electric moments of S_1 interacting with $T_{1,2,3}$ and S_0 . He also developed a method of finding predissociated dark levels and used this information to determine an upper bound for the dissociation energy of acetylene. The

large number of anticrossings found in $3\nu_3$ could not be due to a simple T_3 - S_1 curve crossing because the density of T_3 vibrational levels is not large enough; Green hypothesized that it must be a possible *cis-trans* isomerization barrier in the nearby triplet T_1 or T_2 state at similar energies to the $2\nu_3$ ' \tilde{A} state. The *cis-trans* isomerization barrier is known to lie nearby in energy to the onset of the large number of anticrossings. Only T_1 would have a large enough density of states at energies near $3\nu_3$ to cause the large number of anticrossings.

In a series of *Chemical Physics* papers, Patrick Dupré *et. al.* reported Zeeman Anticrossing (ZAC) experiments on acetylene [13, 11, 12, 10]. In those experiments, they observe a hierarchy of coupling strengths between pairs of the different triplet and singlet excited states. In the first paper in 1991, Dupré, Jost, Lombardi, Green, Abramson, and Field recorded ZAC spectra for the $J=K=I=0$ \tilde{A} state of acetylene for $n\nu_3$ ' ($n = 0-3$) with magnetic field strength of 0-8T [13]. They observed a rapid increase in the number of anticrossings near the $3\nu_3$ ' level. This rapid increase in anticrossings is much larger than would be expected by the increase in density of nearby triplet states [13]. The density of anticrossings observed would only be consistent with the density of highly excited vibrational levels of S_0 . This led Dupré *et. al.* to hypothesize that there must be a mechanism of increasing coupling between the $S_1 \sim T_{1,2}$ levels, possibly due to being near the top of the *cis-trans* isomerization barrier. The triplet levels are then coupled to S_0 by spin-orbit coupling. They assert that the $S_0 \sim T$ coupling is smaller than the $S_1 \sim T$ coupling due to the larger vibrational overlap between S_1 and T since they are closer together in energy than S_0 and T .

In a subsequent paper, Dupré and Green examined the broadest (i.e. strongest) anticrossing in the previously recorded Zeeman anticrossing spectra [11]. For this large anticrossing, the coupling matrix element was relatively large, 3.3 GHz, and had a Landé g-factor of approximately two, indicating that the coupling was to a pure triplet state. For the anticrossings with small coupling matrix elements, the Landé g-factor was found to be less than two, indicating that the coupling was not pure singlet-triplet coupling but a singlet interacting with a perturbed triplet level.

In the third paper of the series, Dupré, Green, and Field analyzed in detail the quantum beat and Zeeman anticrossing spectroscopy of $J=K=N=I=0$ $\tilde{A}^1A_u \nu_3 = 0-2$ and $J=K=N=1, I=0$ $\tilde{A}^1A_u \nu_3 = 0$ levels with magnetic field strengths varying between 0-8 T [12]. They also observed that only a few of the anticrossings had Landé g-factors of two, indicating that most of the anticrossings were due to interaction with a triplet state that was perturbed by yet another triplet state (probably $T_1 \sim T_2$ couplings). Here they generate the ordering of the strengths of coupling: $T_1 \sim T_2 \gg S_1 \sim T \gg S_0 \sim T \gg S_0 \sim S_1$. Later Bittinger also added to this hierarchy: $S_1 \sim T_3 \gg S_1 \sim T_{1,2}$ [5]. In the final paper of the series, Dupré used Fourier transform to determine the anticrossing densities and the average anticrossing half line-width. With this information and the assumption that the coupling is primarily singlet-triplet spin-orbit coupling, Dupré was able to calculate the product $\rho_{vib} \langle V \rangle$ for many rotational levels of the $\tilde{A}^1A_u \nu_3 = 0-4$ states [10]. The product is the density of coupled vibrational levels times the averaged coupling matrix element. He observed this product to increase exponentially with increasing excitation energy and hypothesized this increase to be due to a *trans-cis* isomerization barrier.

In 1994 Drabbels, Heinze, and Meerts carried out a high resolution laser-induced fluorescence experiment on acetylene, examining the $3\nu_3$ and $4\nu_3$ vibrational levels for the S_1 state [9]. They used the Lawrance and Knight spectral deconvolution procedure [24] in order to calculate the singlet-triplet coupling matrix elements, as well as the density of coupled triplet states. From this information they were able to conclude that the \tilde{A} state is perturbed by T_1 (although this is later generalized to T_1 or T_2 [11]). From their magnetic field measurements, they observed that the lines had large magnetic moments, which indicates that the perturbers are triplet states. They also concluded that the triplets can couple not only to the S_1 state, but to high-lying vibrational levels of the ground state.

Acetylene has also been studied using SEELEM (surface electron ejection by laser excited metastables). This detection method is essentially identical to that used by Klemperer and coworkers described above [17], with the variation that SEELEM detects metastables prepared by laser excitation. In 1997 Humphrey, Morgan, Wodtke, Cunningham, Drucker, and Field recorded LIF and SEELEM spectra of acetylene [18]. They observed the intersystem crossing in acetylene to be due to a coupling of the singlet S_1 level to the S_0 level via a triplet intermediate and termed this mechanism as “doorway-mediated coupling.” In 2000 Altunata and Field applied statistical methods to analyze SEELEM spectra in relation to LIF spectra [3], first applying the method to acetylene. These statistical methods can be applied to the spectra to differentiate between this “doorway-mediated coupling” mechanism and a direct coupling scheme. Virgo, Bittinger, Steeves, and Field have recorded the most recent acetylene SEELEM spectra

[5, 43]. They have applied a new technique called “Late-gated fluorescence” to analyze their spectra. This will be discussed in more detail in Chapter 5.

1.3 Previous Theoretical Work on Acetylene

The first modern *ab initio* calculations on acetylene were performed by Kammer in 1970 [21]. In that work, Kammer predicted stable conformations for both *cis* and *trans* isomers for almost every low-lying excited state of acetylene.

In 2003 Ventura, Dallos, and Lischka carried out extended multireference electron correlation calculations on the S_1 , S_2 , and $T_1 - T_4$ states of acetylene [42]. By using this general multireference method, they were able to calculate minima and saddle points for high lying electronically excited states, and their findings compared well to experimental results. They observed that most of the states studied were stabilized by *cis* or *trans* bending, and T_3 and T_4 were in addition particularly stabilized by the out-of-plane torsion. In this study, they also analyzed three potential energy surface curve crossings: S_1/S_2 , T_2/T_3 , and S_1/T_3 .

Ventura and coworkers observed that S_1 had very well established *cis* and *trans* minima, as well as linear and nonlinear saddle points [42]. S_2 has a very shallow *trans* minimum and a *cis* saddle point; however, the true minimum is of C_s symmetry. They found that near the saddle point in the *cis*- C_{2v} geometry, with increasing quanta in the antisymmetric bend, the S_2 energy decreases while the S_1 energy increases, resulting in an intersection very near the C_s minimum of S_2 .

Ventura and coworkers also examined the T_2/T_3 crossing as part of the photodissociation mechanism [42]. They found the torsional mode to have a local minimum on T_3 near the potential energy crossing of T_2 and T_3 . Starting in either the *cis*

or *trans* well, as the torsional displacement increases, the energy of T_3 decreases while that of T_2 increases, resulting in two intersections between T_2 and T_3 . They also examined the effect of vibration in the antisymmetric bend. This was found to lower T_2 while increasing T_3 . Thus there is no crossing, and the state is stable against antisymmetric bending.

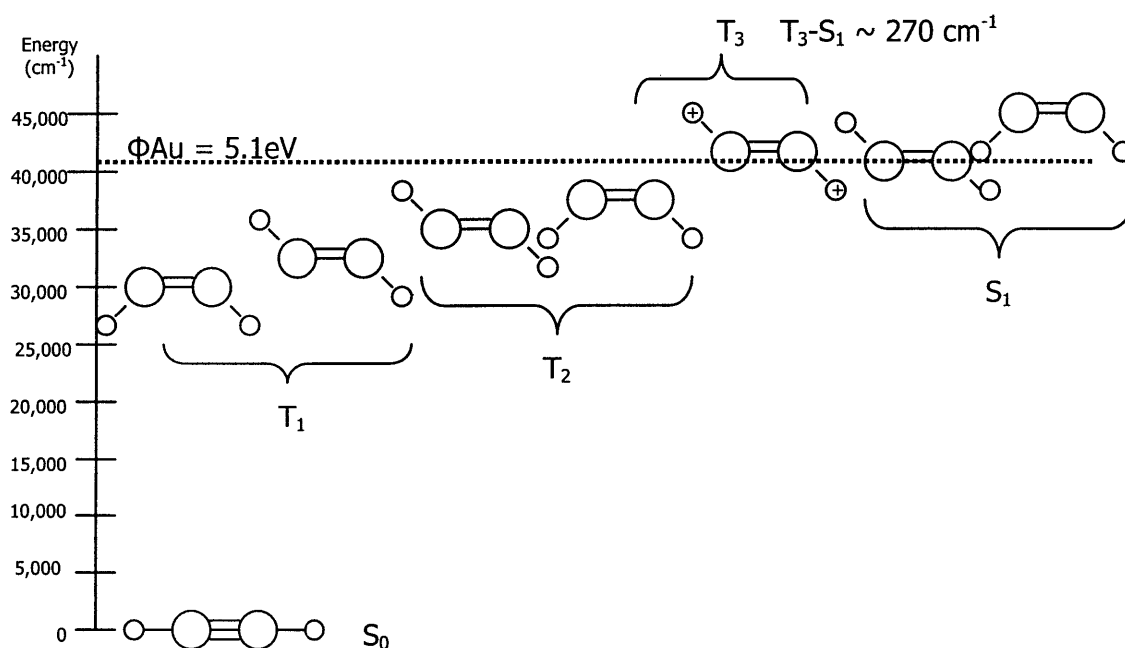
The final surface crossing examined by Ventura and coworkers [42] was the $S_1/T_{2,3}$ crossing speculated from the Zeeman anticrossing studies performed by Dupré [10-13]. From their calculations, they found no surface crossing between S_1 and T_2 as was speculated to be the cause of the increase in anticrossings. However, they found that S_1 and T_3 do have a surface crossing, and this occurs near the energy of the onset of abnormalities in the Zeeman anticrossing spectra.

In 2007 Thom, Wong, Field, and Stanton carried out new *ab initio* calculations to study the T_3 potential energy surface, along with equilibrium geometries and diabatic frequencies [41]. The coupling matrix element between T_3 and S_1 can be factored approximately into an electronic factor and a vibrational overlap factor, each which can be approximately calculated. They were able to compute the vibrational overlap integrals between different T_3 vibrational levels and the S_1 $3\nu_3$ state. The $S_1\sim T_3$ matrix element has been seen to increase from the Zeeman anticrossing experiments with increasing excitation in ν_3 . This is due to an increase in the vibrational overlap factor. The authors hypothesize that this coupling is responsible for the behavior observed in the Zeeman anticrossing experiments [10-13]. They also note, however, that the density of T_3 states alone is not large enough to account for the number of anticrossings observed, so the T_3 state is most likely coupling to the $T_{1,2}$ states. By calculating electronic matrix elements

and vibrational overlap integrals for T_3 vibrational levels near the energy of the S_1 $3\nu_3$ levels, the authors are able to suggest the most likely perturber candidates as being the $2\nu_3 + \nu_4$ and $3\nu_4 + 4\nu_6$ T_3 vibrational levels.

Figure 1.1 shows a summary of the electronic energy levels of the first three triplet states and first excited singlet state of acetylene. For the T_1 state, the *cis* isomer lies lower in energy than the *trans* isomer. For T_2 , T_3 , and S_1 the *trans* isomer lies lower in energy than the *cis* isomer. T_3 and S_1 differ in energy minima by only ~ 270 cm^{-1} .

Figure 1.1: Energy levels for *cis* and *trans* isomers of the low-lying excited states of acetylene



1.4 Vibrational Modes and Electronic Energy Levels of Acetylene

As can be seen from the previous experimental and theoretical work, an understanding of the vibrational modes, geometries, and group theory of acetylene is essential to an understanding of the phenomena described in this thesis. An understanding of the vibrational modes of acetylene is imperative because it is expected that during excitation, as acetylene undergoes an electronic transition from a linear geometry to a bent geometry, there should be progressions in the bending vibration ν_4'' [2]. It is also known that in the excited singlet state the carbon-carbon bond length is 0.18 Å longer than in the ground state. Thus it is also expected that the emission spectrum will have progressions in the CC stretch ν_2'' [2].

The ground state of acetylene is linear in geometry with $^1\Sigma_g^+$ symmetry. The vibrational modes of the ground state are shown in Figure 1.2. The first excited singlet state of acetylene is *trans* bent with 1A_u symmetry. The vibrational modes are shown in Figure 1.3.

Figure 1.2: Vibrational modes of the ground state of acetylene

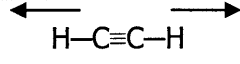
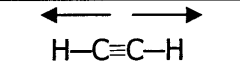
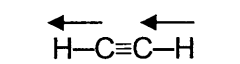
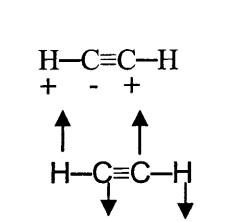
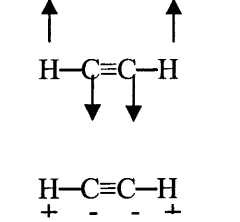
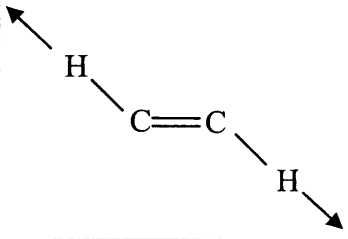
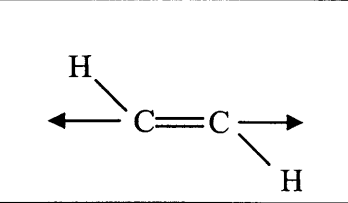
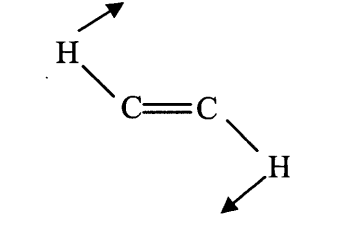
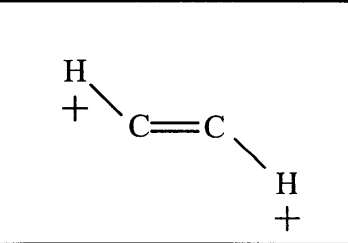
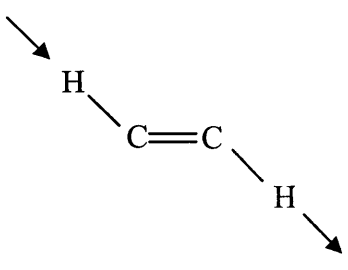
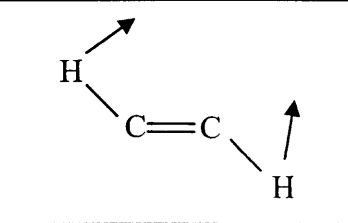
Mode	Description	Symmetry	Normal Mode
ν_1	Symmetric C-H Stretch	Σ_g^+	
ν_2	Symmetric CC Stretch	Σ_g^+	
ν_3	Antisymmetric C-H Stretch	Σ_u^+	
ν_4	Symmetric Bend	Π_g	
ν_5	Antisymmetric Bend	Π_u	

Figure 1.3: Vibrational modes of the first excited singlet state of acetylene

Mode	Description	Symmetry	Normal Mode
ν_1	Symmetric C-H Stretch	a_g	
ν_2	Symmetric CC Stretch	a_g	
ν_3	Symmetric In-Plane Bend (<i>trans</i> Bend)	a_g	
ν_4	Torsion	a_u	
ν_5	Antisymmetric C-H Stretch	b_u	
ν_6	Antisymmetric In-Plane Bend (<i>cis</i> Bend)	b_u	

1.5 Objective of thesis

The previous experimental and theoretical work on acetylene has helped us gain much insight into this molecule. However, it has also raised questions for future work. We have seen that there is a complicated mechanism of coupling in the molecule where S_1 levels couple strongly to T_3 levels, which then couple to the bath of $T_{1,2}$ levels. These $T_{1,2}$ are then coupled to highly vibrationally excited levels of the ground S_0 state. We would like to learn more about this mechanism of coupling of the singlet S_1 state to the triplet T_3 state. Since the state-mixing associated with this coupling is governed by an electronic matrix element and a vibrational overlap integral, along with an energy denominator, we would like to know the nature of the doorway triplet state. Is this triplet vibrational state nearby in energy with a small vibrational overlap integral or distant in energy with a large vibrational overlap integral? Will excitation in particular vibrational modes enhance or diminish the coupling? Does the coupling increase or decrease due to a nearby isomerization barrier or a dissociation pathway? If we are able to answer these questions, we will have learned a great deal of information about the intersystem crossing coupling mechanisms of acetylene. This basic knowledge can, in turn, lead us to a better understanding of larger molecules. For example, the kinds of theories explored here have been applied to larger molecules by Brooks Pate in order to compare the mechanisms of vibrational energy redistribution between gas-phase isolated molecules and solvation effects in condensed phase samples [45].

In this thesis, I will propose a new experiment to explore the answers to these questions about the role of vibrational coupling in intersystem crossing. I will first describe the concepts necessary to understand the methodology: spin-orbit coupling,

radiative lifetimes, the Zeeman effect, and late-gated fluorescence. I will then describe the experimental setup and describe how this method can be used to gain insight into these processes.

Chapter 2: Spin-orbit Coupling

2.1 Theory of spin-orbit coupling

The primary mechanism of interaction between the S_I and T_3 electronic levels is through spin-orbit coupling. Spin-orbit interaction is also responsible for coupling between states of the same spin and is the cause of the $T_3 \sim T_{1,2}$ coupling. Spin-orbit coupling is usually treated as a phenomenological perturbation to the Hamiltonian. Its operator has the form $H_{SO} = \sum_i a_i l_i \cdot s_i$, where a_i is the spin-orbit coupling constant, l_i is the orbital angular momentum of electron i , and s_i is the spin angular momentum of electron i . Stevens and Brand [38] have derived the spin-orbit matrix elements between singlet and triplet states (see Figure 2.1). (Spin-orbit matrix elements are always $\Delta J = 0$.)

Figure 2.1: Spin-orbit Matrix Elements in Terms of the J and K Quantum Numbers of the Singlet State

ΔN	ΔK	$\langle {}^{ev}\Gamma_S NJK H_{SO} {}^{ev}\Gamma_T N' JK' \rangle$
+1	0	$+ [(J - K + 1)(J + K + 1) / (J + 1)(2J + 1)]^{1/2} \langle V_S V_T \rangle \langle H_{SO}(R_z) \rangle$
0	0	$+ \{ K / [J(J + 1)]^{1/2} \} \langle V_S V_T \rangle \langle H_{SO}(R_z) \rangle$
-1	0	$- [(J^2 - K^2) / J(2J + 1)]^{1/2} \langle V_S V_T \rangle \langle H_{SO}(R_z) \rangle$
+1	± 1	$\mp [(J \pm K + 2)(J \pm K + 1) / 4(J + 1)(2J + 1)]^{1/2} \langle V_S V_T \rangle \{ \langle H_{SO}(R_x) \rangle \mp i \langle H_{SO}(R_y) \rangle \}$
0	± 1	$+ [(J \mp K)(J \pm K + 1) / 4J(J + 1)]^{1/2} \langle V_S V_T \rangle \{ \langle H_{SO}(R_x) \rangle \mp i \langle H_{SO}(R_y) \rangle \}$
-1	± 1	$\mp [(J \mp K - 1)(J \mp K) / 4J(2J + 1)]^{1/2} \langle V_S V_T \rangle \{ \langle H_{SO}(R_x) \rangle \mp i \langle H_{SO}(R_y) \rangle \}$

Here the angular momentum quantum numbers are the following: J is the total angular momentum exclusive of nuclear angular momentum, N is the total rotational angular momentum, and K is the absolute value of the projection of N on the z -axis. $\langle V_S | V_T \rangle$ is the vibrational overlap integral, and $\langle H_{SO}(R_\alpha) \rangle$ is the spin-orbit matrix element between the vibronic wavefunctions of the singlet and triplet electronic states with a particular spin component of the triplet ($\langle H_{SO}(R_\alpha) \rangle = \langle \Gamma_S | H_{SO}(R_\alpha) | \Gamma_T \Gamma_\sigma(R_\alpha) \rangle$, where $\alpha = x, y, \text{ or } z$). The molecule-fixed spin functions transform as the $x, y, \text{ and } z$ components of a rotation in the point group of the molecule which leads to the use of R_α . As can be seen from the figure, the spin-orbit matrix element depends on rotational, vibrational, and electronic factors.

2.2 Application to experiment

For the experiments, choose a particular $J=K=N=0$ vibrational level of the singlet to excite. Since N and K are nonnegative, only ΔN and $\Delta K = 0, +1$ perturbations are allowed for this case. From Figure 2.1, one can see that for $\Delta N = 0 \Delta K = 0$, so $H_{SO} = + \{K/[J(J+1)]^{1/2}\} \langle V_S | V_T \rangle \langle H_{SO}(R_z) \rangle = 0$ since $K = 0$. Also, for $\Delta N = 0 \Delta K = +1$, $H_{SO} = +[(J \mp K)(J \pm K + 1)/4J(J+1)]^{1/2} \langle V_S | V_T \rangle \{ \langle H_{SO}(R_x) \rangle \mp i \langle H_{SO}(R_y) \rangle \} = 0$ since $J - K = 0$. This leaves only two possible nonzero matrix elements: $\Delta N = 1, \Delta K = 0$ or 1 . For $\Delta N = 1, \Delta K = 0$,

$$H_{SO} = \langle V_S | V_T \rangle \langle H_{SO}(R_z) \rangle,$$

and for $\Delta N = 1, \Delta K = 1$,

$$H_{SO} = (1/\sqrt{2}) \langle V_S | V_T \rangle [\langle H_{SO}(R_x) \rangle \mp i \langle H_{SO}(R_y) \rangle].$$

These two possibilities result in restrictions on the vibrational symmetry of the triplet level, since for $\Delta K = 0$, the spin-vibronic symmetries of the two states must be related by a rotation about the z axis, while for $\Delta K = 1$, the spin-vibronic symmetries must be related by a rotation about the x or y axes. One can also see that the matrix element is a product of the vibrational overlap integral and the electronic matrix element. The vibrational overlaps can be calculated relatively accurately; however, electronic matrix element calculations may be incorrect by a much larger percentage. By looking at particular $J=K=N=0$ levels of different vibrational states, the analysis of spin-orbit coupling will be simplified since there are only 2 possible rotational levels of each vibrational triplet state that can interact with the singlet.

2.3 Method to access $J = K = N = 0$ states experimentally

From the preceding two sections it has been shown that if one can access exclusively the $J = K = N = 0$ states experimentally, the spectroscopic analysis will be much greatly simplified. A laser excitation scheme has been employed previously in order to access these states [30, 37, 36]. Because the electronic $\tilde{A}-X$ transition in acetylene is a c -type transition, it has the selection rule $K' - l'' = \pm 1$, where K' is the absolute value of the projection of N on the z -axis in the upper state and l'' is the vibrational angular momentum in the lower state. Therefore, in order to access the $K = 0$ states, one must begin in an $l'' = 1$ ground state. ν_4'' (π_g symmetric bend) and $\nu_3'' + \nu_4''$ (π_u antisymmetric C-H stretch and symmetric bend) are $l'' = 1$ states. By starting in these vibrational levels of the ground state (or by gaining access to them using an IR transition

from the vibrationless ground state), one can induce electronic transitions into the $K' = 0$ level of the excited state.

The vibrational selection rules for this $u \leftrightarrow g$ transition are $u \leftrightarrow u$ and $g \leftrightarrow g$. Thus by choosing a *gerade* vibrational level of the ground state, one can gain access to *gerade* vibrational levels of the excited state. Likewise by choosing *ungerade* levels of the ground state, one can observe *ungerade* vibrational levels of the excited state.

To summarize, one can spectroscopically observe the $K = 0$, *gerade* vibrational levels of the \tilde{A} excited electronic state by a one-photon UV transition from the ν_4'' vibrational level (hot band) of the ground electronic state. To examine the $K = 0$, *ungerade* vibrational level of the \tilde{A} excited electronic state, an IR-UV two-photon transition must be employed to first excite the molecule from the vibrationless ground state into the $\nu_3'' + \nu_4''$ vibrationally excited level of the ground electronic state, followed by transition from this intermediate state into the excited electronic state. Population in the vibrationally excited levels of the ground state can be achieved experimentally by exciting the molecular beam closer to the nozzle and adjusting the laser pulse to coincide with the beginning of the nozzle pulse.

Chapter 3: Radiative Lifetimes

3.1 Theory of radiative lifetimes

The basis for the theory of radiative transitions was described by Mulliken [28]. Mulliken described a theory to account for the transition strengths in electronic transitions. Mulliken defines the absorption coefficient k_ν according to

$$I_\nu = I_\nu^0 e^{-k_\nu l} \quad (\text{Eq. 3.1})$$

where I_ν is the radiation at frequency ν that passes through a sample, I_ν^0 is the radiation at frequency ν incident on the sample, and l is the pathlength through the sample. (This equation assumes the sample is at 0°C and 1 atmosphere pressure.) Mulliken also defines the dipole strength D' for the transition involving the orbital electronic wave functions ψ' and ψ'' as

$$D' = Q'^2, \text{ with } Q' = \int \psi'^* (\sum_i q_i) \psi'' d\tau, \quad (\text{Eq. 3.2})$$

where q_i is one coordinate (x , y , or z) of the i th electron. The Einstein probability coefficients per molecule are then given by

$$A' = [64\pi^4 \nu^3 e^2 / 3h] G'' D' \quad (\text{Eq. 3.3})$$

$$B'' = [8\pi^3 e^2 / 3h^2 c] G' D' \quad (\text{Eq. 3.4})$$

where A' is the Einstein A coefficient (total spontaneous emission probability), ν is the frequency of radiation, and G is the number of suitable final orbitals belonging to the same final energy level with which any one of the initial orbitals can combine. The radiative lifetime of a molecule is related to the Einstein A coefficient (the spontaneous emission probability) by

$$\tau = 1 / \sum_i A_i . \quad (\text{Eq. 3.5})$$

For a system with N_0 molecules initially promoted to an excited state, their rate of decay occurs according to $N = N_0 \exp(-At)$, where N is the number of molecules remaining in the excited state.

3.2 Application to experiments

Despite this relatively simple method to calculate the radiative lifetime of molecules, it was observed that some molecules have anomalously long lifetimes. By using the approximation that the wavelength range of emitted radiation is small compared to the average wavelength, Douglas expands the Einstein A coefficient equation to

$$A(\nu') = (1/3h)(64\pi^4 G'' e^2 R_e^2 \nu_e^3) \quad (\text{Eq. 3.6})$$

where R_e is the internuclear distance and ν_e is the approximate center of emission [8].

Douglas describes four methods by which the radiative lifetime of a molecule in a collision free environment may be anomalously long. The first method by which a molecule may have an anomalously long lifetime is a consequence of the approximations made to obtain Eq. 3.6. Here it is assumed that the molecule has a fixed internuclear distance, so the summation over Franck-Condon factors is equal to one. If two potential curves have different shapes, only Franck-Condon factors for downward transitions at a few wavelengths will be appreciable, and this summation will not be equal to one, making the actual lifetime longer than naively expected.

A second mechanism where the lifetime may be different from that calculated is when an excited molecule undergoing large amplitude vibrations approaches dissociation. The third mechanism occurs when vibrational states are mixed; overlap integrals

involving different modes of vibration will tend to force the molecule to radiate at a frequency low compared to the mean frequency assumed in Eq. 3.6.

The fourth and most important mechanism for this discussion is interelectronic level mixing. Suppose one has a three level system, X, A, and B, where $B \leftarrow X$ is allowed but $A \leftarrow X$ is not. In addition, suppose that A and B are strongly coupled due to a high vibrational density of A levels in the vicinity of B. Then when one promotes a transition from X to B, the states of B will mix strongly with those of A, and since A cannot radiate back to the ground state, the radiative lifetime of B will become lengthened. When the density of A levels is very high, B is essentially “diluted” into many of the levels of A.

Spin-orbit coupling between the S_1 and T_3 states of acetylene will lengthen the radiative lifetime of S_1 by exactly this last mechanism. This is indeed observed in the ν_3' = 1-4 states as reported in the Introduction. Measurement of the radiative lifetime will allow one to pinpoint levels that are mixing with triplets, to approximate the mixing fraction, and to observe quantum beats. These phenomena will be discussed in the following chapter on the Zeeman effect.

Chapter 4: Zeeman Effect

4.1 Theory of the Zeeman Effect

Lombardi has described the theory of the Zeeman effect in detail as it relates to analyzing intersystem crossing [28]. Rovibronic states having M_S (the projection of S onto the space-fixed Z axis) not equal to 0 can be shifted by a magnetic field. The magnitude of this shift is given by $M_S g \mu_B B$, where g is the Landé g factor ($g = 2$ for a pure triplet, 0 for a pure singlet), μ_B is the Bohr magneton (9.274×10^{-24} J/T), and B is the magnitude of the applied magnetic field. This derivation will assume a two-level system consisting of a coupled “bright” singlet state $|s\rangle$ and a “dark” triplet state $|t\rangle$ in the presence of a magnetic field where only $|t\rangle$ is Zeeman active. This derivation will also assume that the singlet and triplet levels do not have fine or hyperfine structure and they can only relax by emission of radiation. Let γ_s and γ_t be the pure singlet and triplet radiative lifetimes, respectively, and V_{st} is the coupling strength between the two states.

The Hamiltonian for this system is

$$H = \begin{vmatrix} E_s & V_{st} \\ V_{st} & E_t \end{vmatrix} = \begin{vmatrix} E_s^0 & V_{st} \\ V_{st} & E_t^0 + mg\mu_B B \end{vmatrix} \quad (\text{Eq. 4.1})$$

where E_s^0 is the zero field energy of $|s\rangle$ and E_t^0 is the zero field energy of $|t\rangle$. Solving for the eigenvalues gives

$$E_{1,2} = \frac{1}{2}(E_s + E_t \pm \sqrt{4V_{st}^2 + \Delta E^2}) \quad (\text{Eq. 4.2})$$

where ΔE is given by the following:

$$\Delta E = E_t - E_s = mg\mu_B (B - B_0). \quad (\text{Eq. 4.3})$$

B_0 is the anticrossing magnetic field strength (the field strength at which the two levels $|s\rangle$ and $|t\rangle$ cross and is given by

$$B_0 = (E_s^0 - E_t^0) / mg\mu_B. \quad (\text{Eq. 4.4})$$

Solving for the eigenvectors gives

$$|1\rangle = \alpha|s\rangle + \beta|t\rangle \quad (\text{Eq. 4.5})$$

$$|2\rangle = -\beta|s\rangle + \alpha|t\rangle$$

where α and β are as follows:

$$\alpha = \cos(\theta/2) \quad (\text{Eq. 4.6})$$

$$\beta = \sin(\theta/2)$$

$$\tan(\theta) = 2V_{st} / \Delta E = 2V_{st} / mg\mu_B (B - B_0).$$

One can also define decay rates for the states $|1\rangle$ and $|2\rangle$:

$$\gamma_1 = \alpha^2\gamma_s + \beta^2\gamma_t \quad (\text{Eq. 4.7})$$

$$\gamma_2 = \beta^2\gamma_s + \alpha^2\gamma_t.$$

4.2 Quantum Beat Experiment

In a quantum beat experiment, the molecules are excited by a short [$T < \hbar/(E_1 - E_2)$] laser pulse. This laser pulse creates a coherent excitation between the mixed states $|1\rangle$ and $|2\rangle$. Because the $|s\rangle$ and $|t\rangle$ states are coupled, the population will oscillate between the two states. This creates a fluctuation in the observed fluorescence intensity because only the $|s\rangle$ state can fluoresce. This phenomenon is termed quantum beats.

To derive an expression for the fluorescence decay, first write the initial state of the system. Since the transition to the $|t\rangle$ state is forbidden, initially there is only population in the $|s\rangle$ state.

$$\psi(0) = |s\rangle = \alpha|1\rangle - \beta|2\rangle \quad (\text{Eq. 4.8})$$

By applying the time evolution operator to Eq. 4.8, one obtains

$$\psi(t) = [\alpha \exp(-\alpha_1 t)]|1\rangle - [\beta \exp(-\alpha_2 t)]|2\rangle \quad (\text{Eq. 4.9})$$

where

$$\alpha_i = \frac{1}{2} \gamma_i + i\Delta E. \quad (\text{Eq. 4.10})$$

By substituting in the expressions in terms of $|s\rangle$ and $|t\rangle$ for $|1\rangle$ and $|2\rangle$, one obtains:

$$\psi(t) = [\alpha^2 \exp(-\alpha_1 t) + \beta^2 \exp(-\alpha_2 t)]|s\rangle + \alpha\beta[\exp(-\alpha_1 t) - \exp(-\alpha_2 t)]|t\rangle. \quad (\text{Eq. 4.11})$$

Since the fluorescence intensity is only proportional to the fractional character of $|s\rangle$, taking the square of the coefficient of $|s\rangle$ gives the fluorescence intensity

$$I_F = \alpha^4 \exp(-\gamma_1 t) + \beta^4 \exp(-\gamma_2 t) + 2\alpha^2 \beta^2 \exp[-\frac{1}{2}(\gamma_1 + \gamma_2)t] \cos[(E_1 - E_2)t]. \quad (\text{Eq. 4.12})$$

From Eq. 4.12 it can be seen that the fluorescence is modulated (quantum beats) at a frequency given by the energy difference between the mixed states $|1\rangle$ and $|2\rangle$ ($E_1 - E_2$). This quantum beat modulation frequency can be measured for many values of the magnetic field strength and fitted to the following equation

$$E_1 - E_2 = \sqrt{4V_{st}^2 + [M_s g \mu_B (B - B_0)]^2}, \quad (\text{Eq. 4.13})$$

in order to obtain the coupling between the state (V_{st}), the Landé g-factor ($M_s g$), and the anticrossing magnetic field strength (B_0).

It is important to note that quantum beats can be observed without the presence of a magnetic field. This occurs when two already near-degenerate states are coupled. Zero-field quantum beats will have the same form as given in Eq. 4.12. In this case, $E_1 - E_2 = E_t - E_s$. It should also be noted that near-degenerate states that are not coupled may still be simultaneously populated due to the spectral width of the laser, provided that both have nonzero transition strength from the ground state. In this case the expression for the fluorescence intensity will be given by

$$I_F = \alpha^4 \exp(-\gamma_1 t) + \beta^4 \exp(-\gamma_2 t). \quad (\text{Eq. 4.14})$$

This expression is almost identical to that given in Eq. 4.12, excluding the oscillating term.

It is also possible to use the fluorescence intensity equation to approximate the mixing fraction between singlet and triplet states. Let's assume the quantum beat frequency is too high to observe. Then the fluorescence intensity is approximately given by Eq. 4.14. Secondly let's assume that the states are weakly mixed so that $\alpha^4 \gg \beta^4$. Then the fluorescence intensity is approximately

$$I_F = \alpha^4 \exp(-\gamma_1 t), \quad (\text{Eq. 4.15})$$

and the apparent fluorescence rate is

$$\gamma_1 = \alpha^2 \gamma_s + \beta^2 \gamma_t. \quad (\text{Eq. 4.16})$$

Since $\alpha^2 = 1 - \beta^2$ and γ_s and γ_t can be approximated, one can gain an approximate value for the mixing fraction.

Chapter 5: Late-gated Fluorescence

5.1 Guaranteed Crossings

In his thesis, Kyle Bittinger describes a new method of analysis that can be used to examine distant doorway states [5]. The previous experimental and theoretical work described in the Introduction indicates that S_1 couples to distant vibrational levels of T_3 (the doorway state) which then couple to dense manifold of vibrational levels of $T_{1,2}$. The energies of the rovibrational states of S_1 and T_3 in acetylene can be written as

$$E_{S_1}(\nu, K, J) = T_\nu + [A_\nu - B_\nu]K^2 + \frac{B_\nu + C_\nu}{2}J(J+1) \quad (\text{Eq. 5.1})$$

and

$$E_{T_3}(\nu, K, N) = T_\nu + [A_\nu - B_\nu]K^2 + \frac{B_\nu + C_\nu}{2}N(N+1), \quad (\text{Eq. 5.2})$$

where T_ν is the rotationless energy of the ν vibrational state and A_ν , B_ν , and C_ν are the rotational constants. For T_3 there will be three closely spaced rovibrational states due to the three spin components.

From the spin-orbit selection rules given in Figure 2.1, $\Delta J = 0$, $\Delta N = 0, \pm 1$, and $\Delta K = 0, \pm 1$. Each J level of the singlet can mix with three N levels ($N = J_s, J_s \pm 1$) of the triplet. The energies of these three triplet rovibrational levels is given by

$$E_T(J) = T_{0,T} + \begin{cases} B_T(J+1)(J+2) & \Delta N = +1 \\ B_T J(J+1) & \Delta N = 0 \\ B_T J(J-1) & \Delta N = -1 \end{cases} \quad (\text{Eq. 5.3})$$

The energy of the singlet rovibrational level is given by

$$E_S(J) = T_{0,S} + B_S J(J+1). \quad (\text{Eq. 5.4})$$

If we assume that the rotational constants B_T and B_S are approximately the same, we can calculate the difference in energy between the singlet and triplet levels.

$$\Delta E_{ST}(J) = \Delta T_0 + \begin{cases} 2B_T J + 2B_T & \Delta N = +1 \\ 0 & \Delta N = 0 \\ -2B_T J & \Delta N = -1 \end{cases} \quad (\text{Eq. 5.5})$$

As J increases, the $\Delta N = 0$ triplet state does not move in energy with respect to the singlet state. However, the $\Delta N = \pm 1$ levels move higher or lower in energy relative to the singlet as J is increased. In fact, these triplet energy levels will shift relative to the same- J singlet level by approximately 20 cm^{-1} between the $J = 0$ and $J = 8$ levels. The magnitude of the spin-orbit coupling is governed by the rotational factor, the vibrational factor, the electronic factor, and the energy denominator. The rotational factor does not vary much as J is increased. For a particular pair of vibronic levels of the triplet and singlet, the vibrational and electronic factors will be independent of J . Thus this energy denominator will promote coupling of the singlet to the rotational level of the triplet that lies closest in energy.

Because the magnitude of coupling is governed by the energy difference between the levels and because the triplet levels will be shifted by approximately 20 cm^{-1} , there is a guarantee that there will be a crossing between one of the triplet levels and the singlet level for any two vibrational levels that lie within 20 cm^{-1} of each other. Since one can guarantee a crossing for some $J < 8$ and the coupling is not strongly dependent on the rotational level, one can use this to examine the vibrational dependence of the spin-orbit coupling.

The magnitude of the spin-orbit coupling will determine whether there is a crossing at one particular J or at several values of J . If the magnitude of the spin-orbit

matrix element is on the order of the slope at which the triplet levels are moving ($2B_T$), there will be significant mixing for many values of J . On the other hand if the magnitude of the spin-orbit matrix element is much smaller than $2B_T$, there will be mixing for only one value of J .

5.2 Late-gated Fluorescence

Because of this spin-orbit coupling, mixed singlet-triplet eigenstates will be populated in a laser-induced fluorescence experiment. Due to the difference in lifetimes between the singlet and triplet states, the fluorescence intensity will change as a function of time after the excitation pulse as was discussed in Chapter 4. As a consequence, fluorescence at later time delays will come from states having more triplet character than fluorescence at earlier time delays. Since fluorescence from the triplet states will be at a slightly different frequency than fluorescence from the singlet states, the center of gravity (intensity weighted average frequency) of a peak will shift in energy as the fluorescence is monitored at later times. Because the later fluorescing states are those with more triplet character, the energy shift will be in the direction of the triplet states. This creates a method of determining whether the triplet “doorway” state is higher or lower in energy than the singlet state that it is coupling to. This “late-gated fluorescence” can be used to pinpoint rotational levels of the singlet that are being perturbed by a triplet level and to determine the relative energy ordering of the two states. Whether there is a shift in center of gravity at one J value or at many J values also gives an approximation to the order of magnitude of the spin-orbit coupling matrix element because if the coupling is weak, the energy denominator will cause a shift at only one J , while if the coupling is strong, there

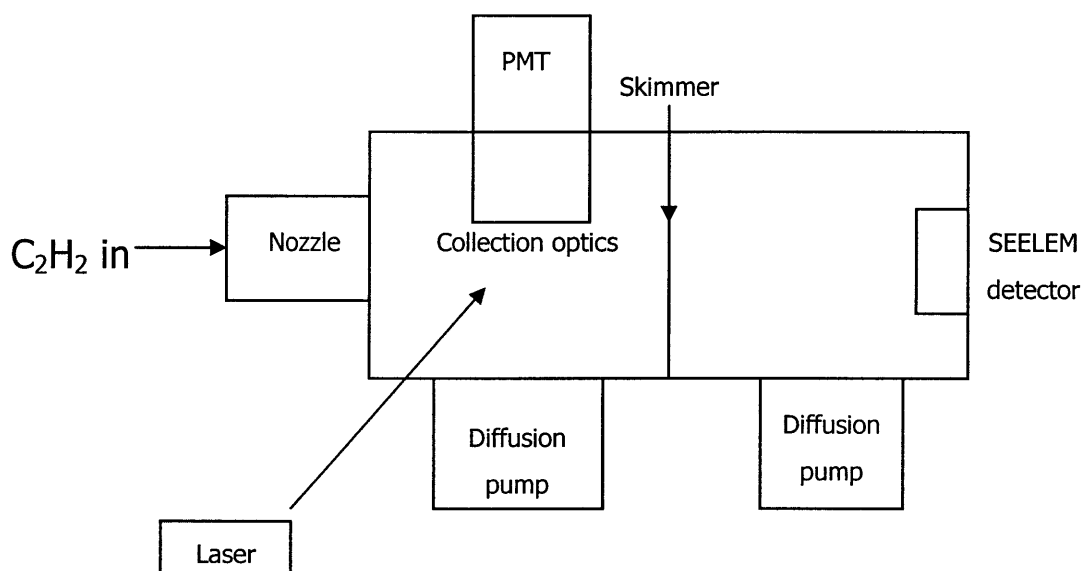
will be shifts for many J values . It is also important to note that one can use late-gated fluorescence to gain information about the doorway state, even if the doorway is too distant in energy to be observed using quantum beats.

Chapter 6: Experimental Details

6.1 Setup of apparatus

Figure 6.1 shows the experimental apparatus.

Figure 6.1: Experimental Apparatus



1 photon UV or
2 color IR-UV

The experiment is performed in a vacuum chamber operating at $\sim 10^{-6}$ torr. A tank of acetylene gas is attached to a pulsed nozzle (0.5 mm diameter nozzle, Jordan Valve) with a variable backing pressure of approximately 1 atmosphere and a repetition rate of 10 Hz. The nozzle creates a molecular beam of acetylene which enters the chamber and undergoes supersonic expansion. An Nd:YAG (Spectra Physics GCR-270) pumped, frequency-doubled dye laser (Lambda Physik FL3002) intersects the molecular beam perpendicularly about 3 cm from the nozzle. Short-lived ($\tau < 10\mu\text{s}$) nominally singlet states will undergo fluorescence which is collected by a series of optics and detected by a photomultiplier (Hamamatsu model R375). This fluorescence detection is referred to as laser-induced fluorescence (LIF) spectroscopy. The fluorescence signal is gated over a specific time interval or a series of time intervals for each frequency and displayed on an oscilloscope where the temporal profile is recorded. This signal is passed to a computer where it can be analyzed.

The molecular beam continues through a skimmer (variable size but typically 3mm diameter) and passes into a second chamber where it collides with the SEELEM detector about 34cm downstream. The SEELEM detector consists of a metal surface (typically gold, having a work function of 5.1eV, although different metals may be used) and an electron multiplier. The metal surface is approximately 2.5cm in diameter and is heated to approximately 300°C to prevent the surface from being contaminated. Molecules that are sufficiently high in electronic excitation energy ($>5.1\text{eV} = 41,134\text{ cm}^{-1}$) and are long-lived ($\tau > 300\mu\text{s}$) will cause an electron to be ejected from the SEELEM surface. Electrons will be detected by an electron multiplier (biased at +100V to attract electrons). The electron multiplier signal was passed through a discriminator and

recorded by a multichannel scalar to sum the total number of electrons. This signal was then displayed and recorded on a computer.

6.2 Application of theories to experiment

Several theories have been described that will be combined to create an experiment that will allow examination of the effect of vibrational excitation on spin-orbit coupling strength in acetylene. This experiment will employ the techniques of Laser-Induced Fluorescence and SEELEM spectroscopies described in the previous section.

From the selection rules for spin-orbit coupling, it has been shown that for the rotationless $J = K = N = 0$ level of the singlet state, there will be only two possible rotational levels ($J = 0, N = 1, K = 0$ or 1) of a given vibrational level of the triplet state that can interact with the singlet through this mechanism. By using the excitation scheme described in Section 2,3, one can exclusively look at these rotationless levels of the singlet state and extremely simplify the analysis of spectra. It has also been shown that the spin-orbit coupling matrix elements will only be dependent on the product of the vibrational overlap integral and the electronic matrix element. Thus we will expect vibrational excitation should have an effect on the coupling strength.

By recording a laser-induced fluorescence spectrum and recording the temporal profiles of the fluorescence decay, one may determine the radiative lifetimes at each frequency step of the laser. Examination of the radiative lifetimes will allow one to identify levels that have a longer than expected lifetime, indicating that they are coupling to triplet states.

In addition to allowing recognition of states that are coupling to triplets, the fluorescence decay traces can be fitted to the fluorescence intensity equation (Eq. 4.12). If quantum beats are observed, this is yet another indication that the state is coupling to the triplet and the frequency of the beat modulation gives the energy difference between the two coupled levels. In addition, one can repeat these experiments in the presence of a magnetic field. This Zeeman effect may tune levels closer together in energy and induce coupling. By measuring the beat modulation at many different magnetic field strengths, one can obtain the coupling strength between the two triplet states. One can also employ this fit to obtain the value of M_{sg} , which will give an approximation to the mixing fraction since $g = 0$ for a pure singlet and 2 for a pure triplet.

By simultaneously recording SEELEM spectra, in addition to LIF spectra, one can identify and characterize the metastable, strongly coupled states. From the shift in energy with increasing J of the triplet rotational levels, it is possible to find the coupling strength and crossing J -value between states by looking at different J values. One can also use the late-gated fluorescence to determine whether the perturber triplet states lie higher or lower in energy than the singlet state.

6.3 Choosing vibrational levels

One should begin by recording spectra of the vibrationless level of the S_1 state. This level is expected to have extremely small vibrational overlap with nearby vibrational levels of T_3 , so this spectrum can be used to gain a baseline measurement of the electronic matrix element between S_1 and T_3 . It is expected that the ν_4 torsional mode will enhance coupling due to a greater vibrational overlap with T_3 that is calculated to

have a twisted equilibrium structure. However, this vibrational mode has been found to couple strongly with ν_6 by Coriolis coupling and Darling-Dennison resonance [30, 37, 36]. The ν_6 vibrational mode (antisymmetric in-plane bend) is expected to decrease coupling with the *trans*-bent T_3 structure. The Coriolis coupling matrix elements between ν_4 and ν_6 have been worked out by Merer, Yamakita, Tsuchiya, Steeves, Bechtel, and Field [30] and are given by

$$\langle \nu_4 \nu_6 Jk | H | \nu_4 \nu_6 Jk \rangle = [A - \frac{1}{2}(B + C)]k^2 + \frac{1}{2}(B + C)J(J + 1) \quad (\text{Eq. 6.1})$$

$$\langle \nu_4 \nu_6 Jk \pm 2 | H | \nu_4 \nu_6 Jk \rangle = \frac{1}{4}(B - C)[J(J + 1) - k(k \pm 1)]^{1/2}[J(J + 1) - (k \pm 1)(k \pm 2)]^{1/2}$$

$$\langle \nu_4 + 1 \nu_6 Jk | H | \nu_4 \nu_6 + 1 Jk \rangle = 2iA \xi_{46}^a \Omega k [(\nu_4 + 1)(\nu_6 + 1)]^{1/2}$$

$$\langle \nu_4 + 1 \nu_6 Jk \pm 1 | H | \nu_4 \nu_6 + 1 Jk \rangle = iB \xi_{46}^b \Omega [J(J + 1) - k(k \pm 1)]^{1/2} [(\nu_4 + 1)(\nu_6 + 1)]^{1/2}$$

$$\langle \nu_4 \nu_6 + 1 Jk | H | \nu_4 + 1 \nu_6 Jk \rangle = -2iA \xi_{46}^a \Omega k [(\nu_4 + 1)(\nu_6 + 1)]^{1/2}$$

$$\langle \nu_4 \nu_6 + 1 Jk \pm 1 | H | \nu_4 + 1 \nu_6 Jk \rangle = -iB \xi_{46}^b \Omega [J(J + 1) - k(k \pm 1)]^{1/2} [(\nu_4 + 1)(\nu_6 + 1)]^{1/2},$$

where

$$\Omega = [(\nu_4 / \nu_6)^{1/2} + (\nu_6 / \nu_4)^{1/2}] / 2$$

and $\xi_{46}^{a,b}$ are the *a* and *b* axis Coriolis coupling constants. These matrix elements all have the form $J \bullet G$, so by looking at the $J = 0$ levels, the spectra will be free of Coriolis coupling effects.

In addition to Coriolis coupling, the ν_4 and ν_6 vibrational levels are also coupled by Darling-Dennison resonance. These matrix elements have also been derived by Merer, Yamakita, Tsuchiya, Steeves, Bechtel, and Field [30] and are given by

$$\langle n_a + 2n_b - 2 | H | n_a n_b \rangle = \frac{1}{4} K_{aabb} [(n_a + 1)(n_a + 2)n_b(n_b - 1)]^{1/2} \quad (\text{Eq. 6.2})$$

where

$$K_{aabb} = \frac{1}{4} \phi_{aabb} + \sum_{\alpha} -B_{\alpha} (\xi_{ab}^{\alpha})^2 \frac{(\omega_a + \omega_b)^2}{\omega_a \omega_b} + \frac{1}{8} \sum_k \phi_{kaa} \phi_{kbb} \omega_k \left(\frac{1}{4\omega_a^2 - \omega_k^2} + \frac{1}{4\omega_b^2 - \omega_k^2} \right) - \frac{1}{2} \sum_k \phi_{kab}^2 \frac{\omega_k}{\omega_k^2 - (\omega_a - \omega_b)^2}. \quad (\text{Eq. 6.3})$$

As can be seen, Darling-Dennison resonance only occurs between vibrational levels differing by two quanta of vibration. By looking at single quanta vibrational modes (ν_4 and ν_6), one can analyze the spectra without complications due to Darling-Dennison resonance.

After examination of the ν_4 and ν_6 vibrational modes with only one vibrational quantum in the $J = 0$ rotationless state, one should obtain an understanding of the effect of the promotion or inhibition of coupling due to excitation in these vibrational modes, without complications due to Coriolis coupling and Darling-Dennison resonances. At this point, it would be interesting to probe more complicated vibrational levels such as $3\nu_4$. This vibrational level will be strongly coupled to ν_6 and will form B^3 polyads. However, by previous experiments on the single quantum levels, it may be possible to more fully understand these much more complicated levels.

It has been observed, as was discussed in the Introduction, that increasing quanta in the ν_3 vibrational mode strongly increases the coupling to the triplet state. Because the ν_4 and ν_6 vibrational modes may have a very weak LIF and SEELEM intensities, it may be necessary to look at vibrational levels of the form $3^x 4^y 6^z$ in order to obtain a stronger signal.

Chapter 7: Conclusion

In this thesis I have described the complex electronic structure of acetylene and an experimental method by which to gain more information about the vibrational coupling of the first excited singlet state to the triplet states. There has been a tremendous amount of effort, both experimentally and theoretically, to study acetylene. A mechanism of coupling of the S_1 state to the T_3 state, which is then coupled to the dense manifold of $T_{1,2}$ states, has been observed experimentally. It has also been observed that by exciting certain vibrational modes, the spin-orbit coupling may be increased.

I have described several theories that may be applied to obtain a better understanding of acetylene. The theory of spin-orbit coupling was described, and it was shown that by exciting particular rotationless states, the vibrational states with which these rotationless levels can couple are limited, making analysis of the spectra much simpler. Excitations of these particular states will also prohibit Coriolis coupling, allowing us to look at excitation in the torsional vibrational mode without additional complications. By measuring the radiative lifetimes and fitting the fluorescence decay to Eq. 4.12, one can identify rovibronic levels that are coupling to triplet states, as well as determine the coupling strength, the mixing fraction, and the difference in energy between the coupled levels. By using the Zeeman effect, one can shift levels closer together to induce coupling, allowing one to gain information about levels that are more distant in energy. One can also use the combination of laser-induced fluorescence (LIF) and SEELEM spectroscopies in order to simultaneously compare spectra consisting of states with primarily singlet character and states with a large fraction of triplet character, respectively. One can also use SEELEM to examine doorway states that are too distant

in energy to be observed either by quantum beats or Zeeman spectroscopy. By looking at shifts in the center of gravity in fluorescence gated at different time intervals, one can observe a shift towards the triplet energy. By observing shifts at one particular J value or at many consecutive J values, information about the size of the spin-orbit coupling matrix element may be obtained.

Finally, we can apply this information to examine certain vibrational levels of the singlet. The ν_4 torsional vibration is expected to increase the spin-orbit coupling by increasing the vibrational overlap factor, while ν_6 is expected to inhibit coupling. By looking at selected combination bands, it may be possible to learn about effects of the torsional and antisymmetric in-plane bending vibrational modes without complications from Coriolis coupling and Darling-Dennison resonance.

In conclusion, one can use the theory and experiments described here to gain information about the effect of vibrational excitation on the spin-orbit coupling in acetylene. This knowledge will allow one to gain an understanding of the fundamental processes involved that can then be applied to other potentially larger molecules of interest.

Bibliography

- [1] E. Abramson, R.W. Field, D. Imre, K.K. Innes, J.L. Kinsey. "Fluorescence and stimulated emission $S_1 \rightarrow S_0$ spectra of acetylene: Regular and ergodic regions." *J. Chem. Phys.* **83**, 453 (1985).
- [2] E. Abramson, C. Kittrell, J.L. Kinsey, R.W. Field. "Excitation spectroscopy of the acetylene $\tilde{A}-X$ transition in the 220 nm wavelength region." *J. Chem. Phys.* **76**, 2293 (1982).
- [3] S. Altunata, R.W. Field. "A statistical approach for the study of singlet-triplet interactions in small polyatomic molecules." *J. Chem. Phys.* **113**, 6640 (2000).
- [4] P.F. Bernath. *Spectra of Atoms and Molecules*. Second Edition: Oxford University Press. (2005).
- [5] K.L. Bittinger. "Spectroscopic Signatures of Doorway-Mediated Intersystem Crossing." PhD thesis, Massachusetts Institute of Technology, (2009).
- [6] C.S. Burton, H.E. Hunziker. "Triplet State of Acetylene: Biacetyl Emission from the Mercury Photosensitized Reaction." *J. Chem. Phys.* **57**, 339 (1972).
- [7] K. Cunningham. "The surface ejection of electrons by laser-excited metastables spectroscopy of acetylene." PhD thesis, Massachusetts Institute of Technology, (2000).
- [8] A.E. Douglas. "Anomalously Long Radiative Lifetimes of Molecular Excited States." *J. Chem. Phys.* **45**, 1007 (1966).
- [9] M. Drabbels, J. Heinze, W.L. Meerts. "A study of the singlet-triplet perturbations in the \tilde{A}^1A_u state of acetylene by high resolution ultraviolet spectroscopy." *J. Chem. Phys.* **100**, 165 (1994).
- [10] P. Dupré. "Study of Zeeman anticrossing spectra of the \tilde{A}^1A_u state of the acetylene molecule (C_2H_2) by Fourier transform: product $\rho_{vib} \langle V \rangle$ and isomerization barrier." *Chem. Phys.* **196**, 239 (1995).
- [11] P. Dupré, P.G. Green. "Characterization of a large singlet-triplet coupling in the \tilde{A} state of the acetylene molecule." *Chem. Phys. Lett.* **212**, 555 (1993).
- [12] P. Dupré, P.G. Green, R.W. Field. "Quantum beat spectroscopic studies of Zeeman anticrossings in the \tilde{A}^1A_u state of the acetylene molecule (C_2H_2)." *Chem. Phys.* **196**, 211 (1995).

- [13] P. Dupré, R. Jost, M. Lombardi, P.G. Green, E. Abramson, R.W. Field. "Anomalous behavior of the anticrossing density as a function of excitation energy in the C₂H₂ molecule." *Chem. Phys.* **152**, 293 (1991).
- [14] W.O. Feikema, P. Gast, I.B. Klenina, I.I. Proskuryakov. "EPR characterization of the triplet state in photosystem II reaction centers with singly reduced primary acceptor Q_A." *Biochemica et Biophysica Acta* **1709**, 105 (2005).
- [15] P.G. Green. "Acetylene Near Dissociation: Novel Effects of External Fields." PhD Thesis. Massachusetts Institute of Technology, Cambridge, MA (1989).
- [16] H.D. Hagstrum. "Theory of Auger Ejection of Electrons from Metals by Ions." *Phys. Rev.* **96**, 336 (1954).
- [17] J.C. Hemminger, B.G. Wicke, W. Klemperer. "Delocalization of electronic energy in the lowest triplet states of molecules." *J. Chem. Phys.* **65**, 2798 (1976).
- [18] S.J. Humphrey, C.G. Morgan, A.M. Wodtke, K.L. Cunningham, S. Drucker, R.W. Field. "Laser excited metastable states of acetylene in the 5.5-5.7 eV region." *J. Chem. Phys.* **107**, 49 (1997).
- [19] C.K. Ingold, G.W. King. "Excited States of Acetylene: Part I-IV." *J. Chem. Soc.* 2702 (1953).
- [20] K.K. Innes. "Analysis of the Near Ultraviolet Absorption Spectrum of Acetylene." *J. Chem. Phys.* **22**, 863 (1954).
- [21] W.E. Kammer. "Ab initio SCF and CI calculations of linear and bent acetylene." *Chem. Phys. Lett.* **6**, 529 (1970).
- [22] M. Kasha. "The Triplet State." *J. Chem. Ed.* **61**, 204 (1984).
- [23] G.W. King, C.K. Ingold. "The Bent Excited State of Acetylene." *Nature* **169**, 1101 (1952).
- [24] W.D. Lawrance, A.E.W. Knight. "Direct deconvolution of extensively perturbed spectra: the singlet-triplet molecular eigenstates spectrum of pyrazine." *J. Phys. Chem.* **89**, 917 (1985).
- [25] G.N. Lewis, M. Kasha. "Phosphorescence and the Triplet State." *J. Amer. Chem. Soc.* **66**, 2100 (1944).
- [26] G.N. Lewis, D. Lipkin, T.T. Magel. "Reversible Photochemical Processes in Rigid Media. A Study of the Phosphorescent State." *J. Amer. Chem. Soc.* **63**, 3005 (1941).

- [27] J.M. Lisy, W. Klemperer. "Electric deflection studies of metastable acetylene." *J. Chem. Phys.* **72**, 3880 (1980).
- [28] M. Lombardi. "Singlet-triplet coupling in small organic molecules by anticrossing, quantum beat, and magnetic resonance spectroscopy." In E.C. Lim and K.K. Innes, editors, *Excited States*, volume 7, p.163. Academic Press. (1988).
- [29] J.K. Lundberg, R.W. Field, C.D. Sherrill, E.T. Seidl, Y. Xie, H.F. Schaefer III. "Acetylene: Synergy between theory and experiment." *J. Chem. Phys.* **98**, 8384, (1993).
- [30] A.J. Merer, N. Yamakita, S. Tsuchiya, A.H. Steeves, H.A. Bechtel, R.W. Field. "Darling-Dennison resonance and Coriolis coupling in the bending overtones of the \tilde{A}^1A_u state of acetylene, C_2H_2 ." *J. Chem. Phys.* **129**, 054304 (2008).
- [31] A.P. Mishra, R.L. Thom, R.W. Field. "New S_I state vibrational and $T_{3,2,1}$ spin-rotational assignments in the vicinity of the acetylene $\tilde{A}^1A_u - X^1\Sigma_g^+ V_0^3K_0^1$ band." *J. Mol. Spectrosc.* **228**, 565 (2004).
- [32] R.S. Mulliken. "Intensities of Electronic Transitions in Molecular Spectra." *J. Chem. Phys.* **7**, 14 (1939).
- [33] N. Ochi, S. Tsuchiya. "Quantum Beat Spectroscopy of Zeeman Splitting and Level Anticrossing of Rotationally Selected Acetylene ($\tilde{A}^1A_u 3\nu_3$) Under Weak Magnetic Fields." *Chem. Phys. Lett.* **140**, 20 (1987).
- [34] N. Ochi, S. Tsuchiya. "Rovibronic level structure of electronically excited acetylene (\tilde{A}^1A_u) in a supersonic jet as studied by laser-induced fluorescence and Zeeman quantum beat spectroscopy." *Chem. Phys.* **152**, 319 (1991).
- [35] G.J. Scherer, Y. Chen, R.L. Redington, J.L. Kinsey, R.W. Field. "An unsuspected Fermi perturbation in the acetylene $\tilde{A}^1A_u 3\nu_3$ level." *J. Chem. Phys.* **85**, 6315 (1986).
- [36] A.H. Steeves, H.A. Bechtel, A.J. Merer, N. Yamakita, S. Tsuchiya, R.W. Field. "Stretch-bend combination polyads in the \tilde{A}^1A_u state of acetylene, C_2H_2 ." *J. Mol. Spectrosc.* **256**, 256 (2009).
- [37] A.H. Steeves, A.J. Merer, H.A. Bechtel, A.R. Beck, R.W. Field. "Direct observation of the symmetric stretching modes of \tilde{A}^1A_u acetylene by pulsed supersonic jet laser induced fluorescence." *Mol. Phys.* **106**, 1867 (2008).
- [38] C.G. Stevens, J.C.D. Brand. "Angular momentum dependence of first- and second-order singlet-triplet interactions in polyatomic molecules." *J. Chem. Phys.* **58**, 3324 (1973).

- [39] R.L. Sundberg, E. Abramson, J.L. Kinsey, R.W. Field. "Evidence of quantum ergodicity in stimulated emission pumping spectra of acetylene." *J. Chem. Phys.* **83**, 466 (1985).
- [40] P. Swiderek, M. Michaud, L. Sanche. "Condensed phase electron-energy-loss spectroscopy of the low-lying triplet states of acetylene." *J. Chem. Phys.* **106**, 9403 (1997).
- [41] R.L. Thom, B.M. Wong, R.W. Field, J.F. Stanton. "Studies of intersystem crossing dynamics in acetylene." *J. Chem. Phys.* **126**, 184307 (2007).
- [42] E. Ventura, M. Dallos, H. Lischka. "The valence-excited states $T_1 - T_4$ and $S_1 - S_2$ of acetylene: A high-level MR-CISD and MR-AQCC investigation of stationary points, potential energy surfaces, and surface crossings." *J. Chem. Phys.* **118**, 1702 (2003).
- [43] W.L. Virgo, K.L. Bittinger, A.H. Steeves, R.W. Field. "Contrasting Singlet-Triplet Dynamical Behavior of Two Vibrational Levels of the Acetylene $S_1 2^1 3^1 B^2$ Polyad." *J. Phys. Chem. A* **111**, 12534 (2007).
- [44] H.R. Wendt, H. Hippler, H.E. Hunziker. "Triplet acetylene: Near infrared electronic absorption spectrum of the *cis* isomer, and formation from methylene." *J. Chem. Phys.* **70**, 4044 (1979).
- [45] H.S. Yoo, M.J. DeWitt, B.H. Pate. "Vibrational Dynamics of Terminal Acetylenes: I. Comparison of the Intramolecular Vibrational Energy Redistribution Rate of Gases and the Total Relaxation Rate of Dilute Solutions at Room Temperature." *J. Phys. Chem. A* **108**, 1348 (2004).